



Contents lists available at ScienceDirect

Atherosclerosis

journal homepage: www.elsevier.com/locate/atherosclerosis



A meprin inhibitor suppresses atherosclerotic plaque formation in ApoE^{-/-} mice

Pan Gao^a, Rui-wei Guo^a, Jian-fei Chen^a, Yang Chen^{a,b}, Hong Wang^a, Yang Yu^a, Lan Huang^{a,*}

^a Department of Cardiology, No. 2 Hospital Affiliated to Third Military Medical University, Xinqiao Hospital, Chongqing 400037, China

^b Department of Neurology, No. 3 Hospital Affiliated to Third Military Medical University, Daping Hospital, Chongqing 400042, China

ARTICLE INFO

Article history:

Received 10 November 2008
Received in revised form 27 April 2009
Accepted 27 April 2009
Available online xxx

Keywords:

Atherosclerosis
Plaque
Apoptosis
Mice

ABSTRACT

Meprin is a member of the astacin family of zinc metalloendopeptidases. It is widely distributed in the body, and hydrolyzes and inactivates several endogenous vasoactive peptides, some of which could alter various functions of cells in the arterial wall. We assessed the influence of chronic meprin inhibition by daily administration of actinonin (5 mg/kg body weight per day; i.p.) on the development of atherosclerotic changes in ApoE^{-/-} mice. Mice were fed a high-fat (21% fat), cholesterol-rich (1% cholesterol) Western-type diet for 16 weeks starting at 10 weeks of age. At 20 weeks of age, randomly selected ApoE^{-/-} mice were treated with Western-type diet chow pellets supplemented with commercially available actinonin (meprin-I group) for 6 weeks; the diet of control ApoE^{-/-} mice was supplemented with saline (placebo group).

There was no difference in body weight, hemodynamic data and serum lipids between the two groups at the end of the dietary period. Meprin-I treatment was found to elevate levels of natriuretic peptides (NPs) in plasma and the vascular wall by radioimmunoassay. Meprin-I treatment also decreased plaque volume and suppressed lipid deposition in carotid arteries. Meprin-I treatment reduced production of reactive oxygen species (ROS) and apoptosis (which are associated with atherosclerosis) in the vascular wall. In *in vitro* experiments, meprin-I treatment increased NP function on cell apoptosis, proliferation, and intracellular ROS generation in the THP-1 cell line and primary vascular smooth muscle cells (VSMC). These results suggest that the meprin inhibitor actinonin may have a protective role in atherosclerosis, and that meprin inhibition may be therapeutically useful in atherosclerosis prevention. Suppression of degradation in the arteries of endogenously released NPs (particularly atrial natriuretic peptide and brain natriuretic peptide), or other kinins known to have anti-atherosclerotic actions, may at least partially contribute to the inhibitory effects of meprin-I on atherosclerotic changes.

© 2009 Elsevier Ireland Ltd. All rights reserved.

1. Introduction

Meprin is a member of the astacin family of zinc metalloendopeptidases. It is highly expressed in the kidney, intestinal brush border membranes, and leukocytes and in some cancer cells [1–3]. It consists of two subunits, α and β , which form disulfide-bridged homodimers and heterodimers that differ in oligomerization potentials and substrate specificity. Meprin- α forms heterogeneous multimers and is secreted. Meprin- β restricts the oligomerization potential of meprin to tetramers and attaches meprin oligomers to the plasma membrane. Its substrates include bioactive peptides and extracellular matrix proteins. Meprin proteins have been implicated in cancer and intestinal inflammation [4,5]. Like neutral endopeptidase 24.11 (NEP), meprin could hydrolyze and inactivate several endogenous growth factors, vasoactive peptides, cytokines, and extracellular matrix proteins circulating in peripheral blood or

produced at vascular walls [6,7]. Endothelial meprin could therefore metabolize vasoactive peptides and reduce their local concentrations at the arterial walls, resulting in attenuation of the effects of the peptides on vascular functions [8,9]. Meprin inhibition may potentiate vascular responsiveness to these endogenous vasoactive peptides.

The natriuretic peptide (NP) family has an important role in the regulation of blood pressure homeostasis and salt and water balance [10,11]. Studies have demonstrated that NPs and other factors in the vascular wall are the substrates of meprin, particularly atrial natriuretic peptide (ANP) and brain natriuretic peptide (BNP) (meprin has no effect on C-type natriuretic peptide (CNP) [12]). NPs can also stimulate the endothelial release of vasodilators such as prostaglandins, endothelium-derived relaxing factor(s), and nitric oxide, which can inhibit the proliferation and apoptosis of vascular smooth muscle cells (VSMC), and modulation of the level of reactive oxygen species (ROS) in different cell types [13–16]. These activities have been strongly associated with experimental hypertension, cardiac hypertrophy, thrombosis, restenosis, and atherosclerosis [17–19].

* Corresponding author. Tel.: +86 23 68755601.
E-mail address: huanglan260@126.com (L. Huang).

Considerable evidence suggests that NP signaling may have a direct role in the development of atherosclerosis: most data support the anti-proliferative action of NP on smooth muscle cells (SMCs), suggesting an anti-atherogenic action of NP. Mice lacking the NPs receptor type-A (NPRA) and ApoE (Npr1^{-/-} ApoE^{-/-}) have increased atherosclerosis compared with ApoE-deficient mice that are of the wild-type for Npr1 (Npr1^{+/+} ApoE^{-/-}) [20]. One could therefore expect that a meprin inhibitor could potentiate the vascular actions of NPs or other kinins by inhibition of their degradation at the vascular wall.

This study initially aimed to assess the influence of chronic meprin inhibition by daily administration of the meprin inhibitor actinonin on the development of atherosclerotic changes in ApoE^{-/-}, and then aimed to clarify elevation of the level of NPs contributed to the anti-atherogenic effects of meprin inhibition.

2. Materials and methods

2.1. Animals

Animal experiments were conducted in accordance with institutional guidelines (Third Military Medical University) and the animal protection law for Chongqing City.

Male ApoE^{-/-} mice (C57/Bl6 genetic background; purchased from Beijing University, Beijing, China) were used in this study. Twenty-eight ApoE^{-/-} mice were maintained in a room set at 22 °C with a 12-h light/dark cycle. They received drinking water *ad libitum*.

Mice were fed a high-fat (21% fat), cholesterol-rich (1% cholesterol) diet for 10 weeks starting at 10 weeks of age. At 20 weeks of age, 20 ApoE^{-/-} mice were randomly treated with Western-type diet chow pellets supplemented with commercially available actinonin (Fluka and Sigma–Aldrich, Shanghai, China; 5 mg/kg body weight per day; intraperitoneal injection; meprin-I group (see below for definition); *n* = 10) or saline (placebo group, *n* = 10) for 6 weeks. Briefly, male ApoE^{-/-} mice (body weight, 20–25 g) received actinonin (5 mg/kg body weight), or an equal volume of saline (i.p.) within 24 h. Twelve hours after the last injection, blood was taken under isoflurane anesthesia by puncture of the retro-orbital venous plexus. Blood samples were put on ice for 30 min to clot and then centrifuged (4 °C; 10 min; 3000 rpm). Serum was snap-frozen in liquid nitrogen and stored at –80 °C until further processing. Dosages used in this study were based on previous studies [12,21]. Blood pressures were measured by a computerized tail-cuff system (BP-2000, Visitech Systems, Apex, NC, USA) in conscious animals. Age-matched controls were killed at age 20 weeks (*n* = 8, ApoE^{-/-} mice with high-fat diet for 10 weeks; control group). After 20 or 26 weeks of age, mice were killed, blood was taken, and carotid arteries subsequently perfused with 0.9% NaCl.

2.2. Natriuretic peptide analyses

Natriuretic peptides were measured in snap-frozen carotid arteries and plasma from experimental animals. Levels of natriuretic peptides were measured by RIA commercial kits specific for ANP and mouse BNP (Phoenix Biotech, Beijing, China) according to the manufacturer's instructions.

2.3. Lipid analyses

Plasma was obtained through centrifugation of the blood for 10 min at 5500 × *g* at 4 °C and stored at –80 °C. Total plasma cholesterol and triglyceride concentrations were measured using enzymatic assay (Roche Applied Science, Shanghai, China) on

a Cobas Mira Plus automated analyzer (Roche Applied Science, Shanghai, China).

2.4. Morphology

For morphometric studies, at 26 weeks of age, rats were anesthetized and killed as described above. After killing, mice were perfusion-fixed with 4.5% formaldehyde. The left carotid arteries were dissected and embedded in paraffin as described. Left carotid arteries were serially sectioned (5 μm) and, beginning from a random start site within the first 75 μm, a section was stained every 75 μm with hematoxylin and eosin (H&E). Images were captured with a Leica microscope and lesion area quantified using an image analysis system. Entire right carotid arteries (9-mm long) were excised and placed in Oil-red-O for 5 min. Images of artery plaques were obtained with a digital camera (Sony, Japan).

2.5. Immunohistochemistry

Immunostainings of paraffin sections for Mac-2 and α-SMC-actin were performed to confirm the presence of macrophages and vascular smooth muscle cells (VSMC) in vascular wall and plaques. Paraffin sections (5 μm) were deparaffinized and rehydrated, and then treated with 0.3% H₂O₂ in methanol for 30 min to abolish endogenous peroxidase activity, and with 2% rabbit serum for 30 min to block non-specific antibody binding. Subsequently, sections were incubated overnight at 4 °C with a rat anti-mouse Mac-2 monoclonal primary antibody (1:25 dilution, Santa Cruz, USA), murine smooth muscle actin (1:10 dilution, Santa Cruz, USA). On the second day, after several washes with PBS, the sections were incubated with biotinylated rabbit anti-rat secondary antibody for 30 min, and visualized with DAB kit (Dingguo Biotechnology, Chongqing, China) followed by counterstaining with 10% Mayer's hematoxylin, and finally, mounted in Permount, and examined by light microscopy. Cross-sections were also stained with Masson trichrome to identify collagen.

2.6. Sodium dodecyl sulfate-polyacrylamide gel electrophoresis (SDS-PAGE) zymography analysis

A gelatin substrate was included in the composition of the polyacrylamide/SDS gels (10% gelatin gel). Samples were separated according to their apparent molecular weight by electrophoresis. After electrophoresis, the gel was washed in 2.5% Triton X-100 solution with gentle agitation for 6 h at room temperature. This was followed by replacement with developing buffer (in g/L) containing dH₂O:Tris base 12.1, Tris–HCl 63, NaCl 117, CaCl₂ 7.4, and Brij-35 0.2. The gel was agitated at room temperature for 30 min, placed in fresh developing buffer, and incubated overnight at 37 °C. The gel was stained with 0.5% Coomassie brilliant blue R-250 and de-stained in 5% methanol and 7% acetic acid. To verify the metalloproteinase nature of detected enzymes, identical gels were incubated in the presence of an inhibitor of matrix metalloproteinases (MMPs), edetic acid (30 mmol/L). Results were expressed as percentage of optical density in control group. Gelatinolytic bands were quantified by scanning densitometry with NIH Image software.

2.7. Measurement of production of vascular superoxide and activity of NADPH oxidase

Carotid artery superoxide levels were measured with dihydroethidium (DHE, Beyotime Institute of Biotechnology, Nanjing, China) on serial frozen sections (10 μm). DHE specificity was previously validated using smooth muscle cells exposed to OxLDL. Two serial sections each from actinonin-infused (Meprin-I) and saline-infused (placebo) mice were tested in parallel. One pair of sections

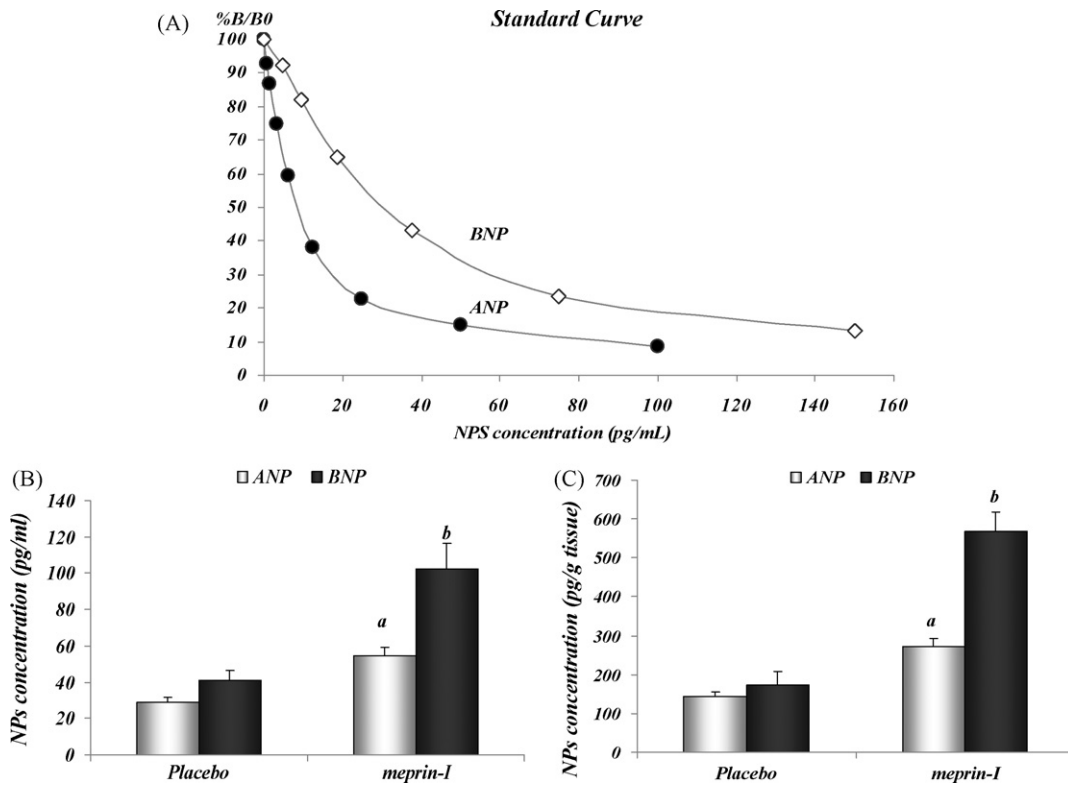


Fig. 1. Content of NPs in plasma and the vascular wall. NP concentration was measured by RIA assay. (A) Standard curves of NP in plasma; (B) concentration of NP in plasma; (C) NP expression in the vascular wall. Data are mean \pm SEM. ^a $P < 0.05$ vs. placebo, ^b $P < 0.01$ vs. placebo.

from actinonin-infused and saline-infused mice was pretreated with superoxide scavenger N-acetylcysteine (NAC, Beyotime Institute of Biotechnology, Nanjing, China) in buffer (50 mmol/L Tris-HCl, pH 7.4), and another pair of sections was preincubated with buffer only. All 4 sections were stained by DHE (2 μ mol/L, 45 min, 37 $^{\circ}$ C) in dark in a humidified chamber, briefly washed, and quickly imaged with a fluorescent microscope keeping the same exposure for every section. DHE fluorescence was quantified by averaging the mean fluorescence intensity within 3 identical circles placed on a plaque-free area of vascular wall using Image-Pro Plus. The superoxide-induced DHE signal was expressed as NAC-inhibitable fluorescence after subtraction of the DHE signal obtained from scavenger-pretreated section. Three to five sections from each animal ($n = 4$ for each saline- or actinonin-infused group) were analyzed using this procedure and the average superoxide-induced DHE fluorescence was calculated.

NADPH oxidase activity in vascular was assessed by lucigenin-enhanced chemiluminescence as described previously with some modifications [22]. Briefly, isolated vessel segments were collected in Krebs-HEPES buffer (composition in mmol/L: NaCl 98.0, KCl 4.7, NaHCO₃ 25.0, MgSO₄ 1.2, KH₂PO₄ 1.2, CaCl₂ 2.5, D-glucose 11.1 and Hepes-Na 20.0, pH 7.4), dissected out the adherent fat and incubated with 3 mmol/L DETCA at 37 $^{\circ}$ C for 45 min to inactivate endogenous Cu/Zn SOD activity. Then tissues were preincubated

with vehicle or bilirubin for 30 min, and NADPH oxidase activity assessed by measuring NADPH (100 μ mol/L)-stimulated superoxide in 300 μ L of Krebs-HEPES buffer containing 5 μ mol/L lucigenin in a 96-well Opti-plate (Packard). Chemiluminescence was detected with a microplate scintillation counter (Topcount model 9912, Packard) running in single-photon-count mode.

2.8. TUNEL

An *in situ* cell death detection POD kit (Roche Applied Science, Shanghai, China) was used with slight modification. Five-micrometer cryosections were pretreated with 3% citric acid, fixed, and labeled according to manufacturer's instructions. After development using diaminobenzidine, sections were counterstained with methyl green. Four serial sections from each mouse were stained. The same protocol was used for terminal deoxynucleotidyl transferase dUTP nick end labeling (TUNEL) of THP-1 macrophages cultured in slides. TUNEL-positive cells were counted in 10 fields under light microscopy (400 \times).

2.9. Cell culture, intracellular ROS production, apoptosis and proliferation

See the data supplement for details.

Table 1

Measurements were obtained before death, 16 weeks after initiation of the diet. Placebo indicates ApoE^{-/-} mice fed a 1% cholesterol diet and supplemented with saline. Meprin-I indicates mice fed a 1% cholesterol diet and supplemented with 5 mg/kg per day of the meprin inhibitor actinonin. Data are mean \pm SEM. BW = body weight; BP = blood pressure; HDL = high-density lipoprotein.

Group	BW (g)	BP (mmHg)	Cholesterol (mg/dL)	Triglyceride (mg/dL)	HDL (mg/dL)
Placebo	32 \pm 0.4	107 \pm 8	372 \pm 24	66 \pm 8	27 \pm 6
Meprin-I	28 \pm 0.5	115 \pm 6	416 \pm 33	75 \pm 14	30 \pm 5
P value	>0.05	>0.05	>0.05	>0.05	>0.05

2.10. Statistical analysis

SPSS13.0 software was used for statistical analysis. All of the experiments were repeated at least 3 times, with similar patterns of results. Data are presented as mean ± SEM. Groups of data were compared with ANOVA followed by Tukey's multiple comparison tests. Values of $P < 0.05$ were regarded as significant.

3. Results

3.1. Accumulation of NP in plasma and vascular tissue

We first aimed to confirm that ApoE^{-/-} administrated with actinonin resulted in increased levels of NPs in plasma and vascular tissues. BNP levels of meprin inhibition (meprin-I) in ApoE^{-/-} mice were significantly increased by 2.5-fold in plasma and 3.3-fold in the vascular wall compared with those observed in ApoE^{-/-} control mice (Fig. 1). ANP levels were also significantly increased by 1.9-fold in plasma and 1.8-fold in the vascular wall (Fig. 1). Total cholesterol, triglyceride levels, body weights and blood pressure were similar in meprin-I ApoE^{-/-} mice and ApoE^{-/-} mice (Table 1).

3.2. Formation of atherosclerotic lesions in ApoE^{-/-} mice

After treatment with a high-cholesterol diet for 10 weeks, atherosclerotic lesions and lipid accumulation were observed in the carotid arteries of ApoE^{-/-} mice (control group, Fig. 2). ApoE^{-/-}

mice fed with 1% cholesterol diet only for 16 weeks showed larger atherosclerotic lesions in carotid arteries compared with control group when cross-sections were stained by H&E (placebo group, Fig. 2A). Treatment with actinonin changed the size of atherosclerotic lesions in carotid arteries compared with placebo group (meprin-I group, Fig. 2A), which suggested actinonin exerted apparent anti-atherogenic actions. These inhibitory effects of actinonin on atherosclerosis were significantly displayed among the three groups when entire right carotid arteries were stained by Oil-red-O (Fig. 2B).

3.3. Lesion composition in ApoE^{-/-} mice treated with or without actinonin

To evaluate lesion composition in the three groups, we immunostained lesions for macrophages, SMCs, as well as collagen and calculated the percentage of lesional area occupied; we examined $n = 40$, $n = 62$ and $n = 55$ sections in the three groups of male mice, respectively. We observed augmentation of macrophage content in lesions of placebo mice ($54.32 \pm 1.74\%$) compared with control group ($32.48 \pm 2.15\%$). Treatment with actinonin reduced macrophage content (decreased to $24.05 \pm 3.42\%$) compared with placebo group. SMC content did not differ significantly between the three groups ($10.32 \pm 0.56\%$ in control group, $8.16 \pm 0.67\%$ in placebo group, and $9.48 \pm 0.90\%$ in meprin-I group). Among the three groups, collagen content was the highest in lesions of meprin-I group ($35.42 \pm 1.20\%$), but collagen content did not show a sig-

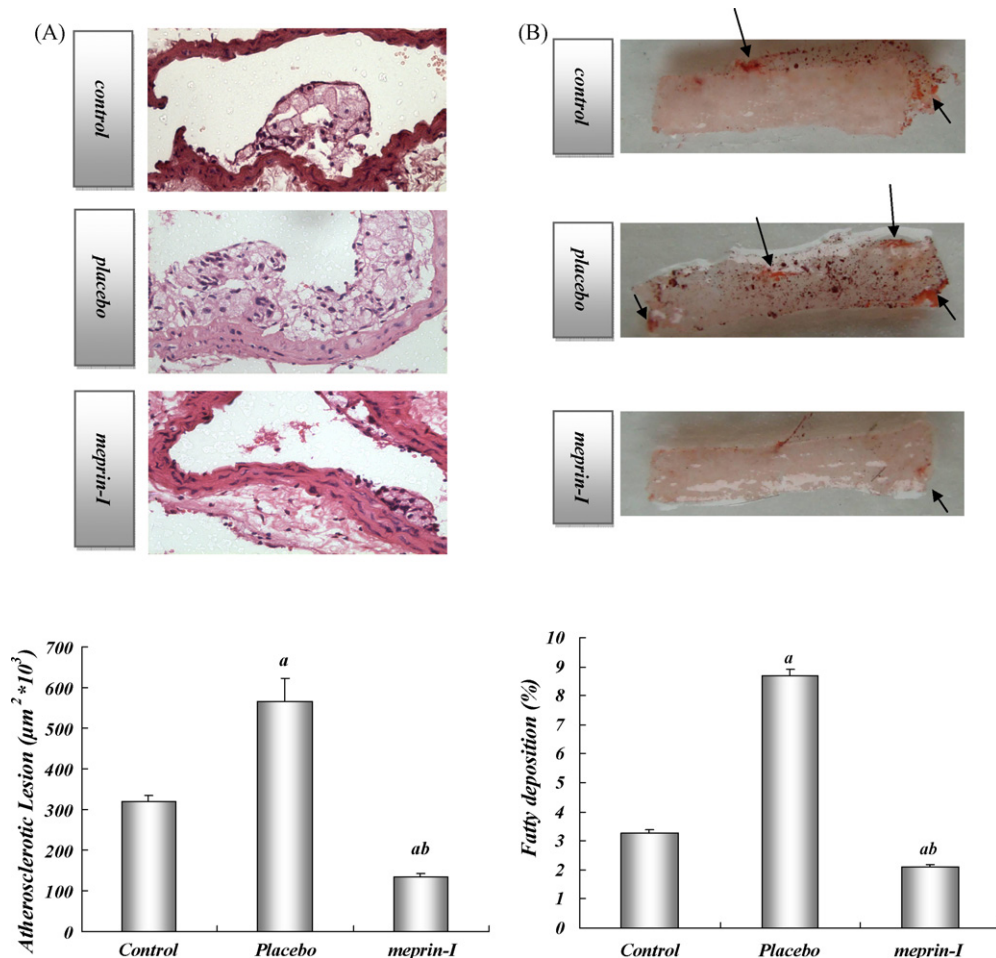


Fig. 2. (A) Cross-sectional aortic lesions. Cryosections of carotid artery stained with H&E in the three groups. (B) En-face aortic lesions. Carotid arteries were stained by Oil-red-O from the three groups. Graphs A and B also show quantitative data in controls, placebo and meprin-I mice (column graph). Data are mean ± SEM. ^a $P < 0.05$ vs. control mice. ^b $P < 0.05$ vs. placebo mice.

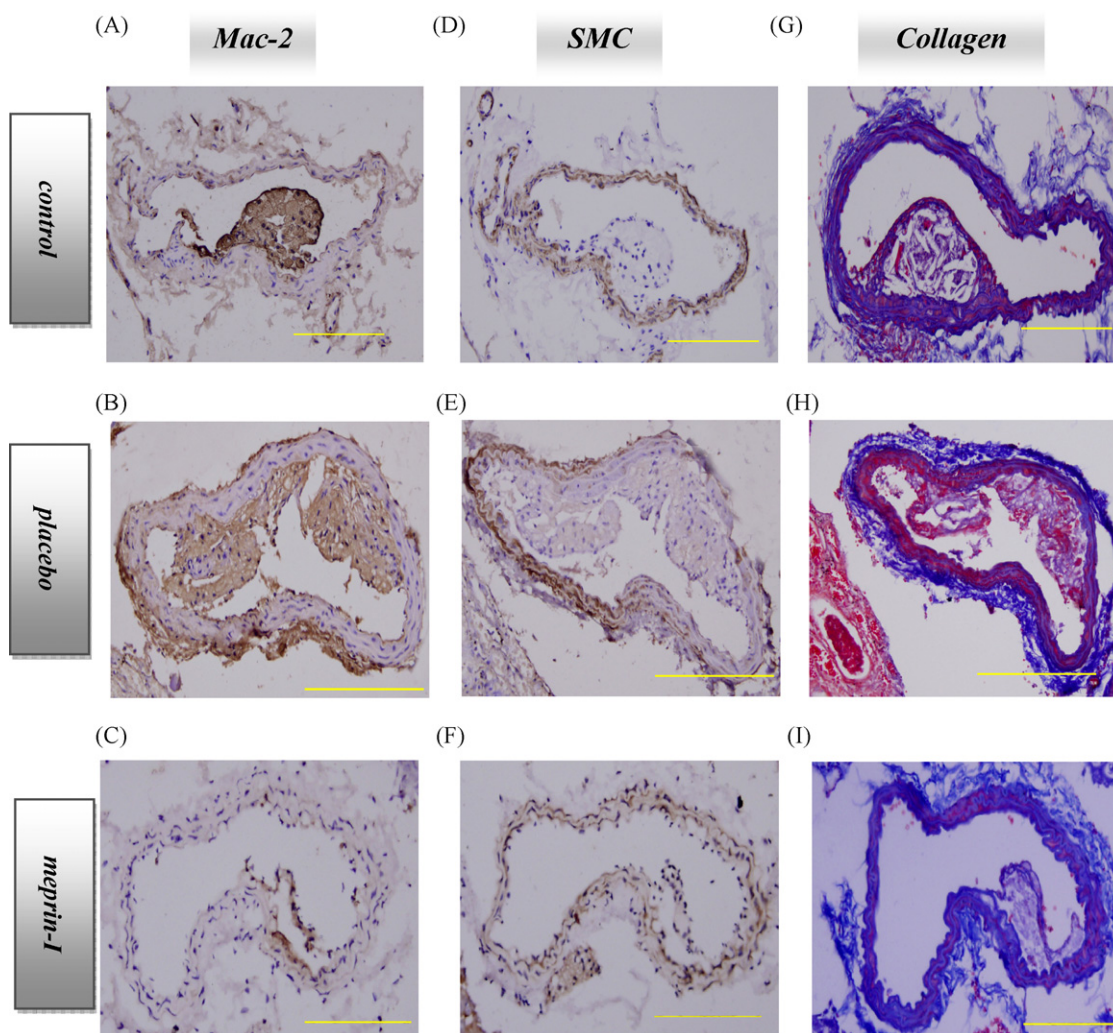


Fig. 3. Composition of atherosclerotic lesions in the carotid arteries of the three groups of ApoE^{-/-} mice. Representative staining for macrophages (anti-Mac-2), SMC (anti- α -SMC-actin) and collagen (Blue, Masson trichrome staining). Bar = 200 μ m.

nificant difference in atherosclerotic lesions of control group and placebo group ($18.72 \pm 2.68\%$ vs. $20.43 \pm 1.03\%$). Compared with the placebo administration, chronic actinonin treatment significantly decreased plaque T cells number (percentage of CD3⁺ cells per total lesion cell number, $P < 0.05$; Supplement figure II). Taken together, treatment of ApoE^{-/-} mice with actinonin resulted in dramatic reduction in lesion size, monocyte/macrophage content, and augmentation of collagen deposition compared with placebo group ($35.42 \pm 1.20\%$ vs. $20.43 \pm 1.03\%$, Fig. 3). These results suggest that treatment with actinonin halted genesis/progression of plaques, and altered the phenotype of lesions in ApoE^{-/-} mice.

3.4. Assay of matrix metalloproteinase-9 (MMP-9) activity

Previous studies have demonstrated that certain MMPs (e.g., MMP-9) were upregulated in ApoE^{-/-} mice fed a high-fat diet [23]. MMP-9 is believed to contribute to the development and progression of atherosclerosis [24]. To clarify the activity of MMP-9 in the three groups, SDS-PAGE zymography analysis was done. In the present study, ApoE^{-/-} mice of placebo group and control group did not display a significant difference in MMP-9 activity. In mice treated with actinonin, MMP-9 activity was significantly reduced compared with placebo (Fig. 4). This result was consistent with actinonin-induced augmentation of collagen deposition.

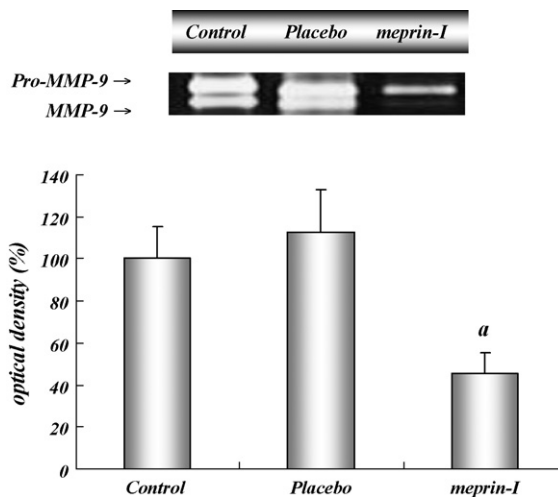


Fig. 4. Determination of MMP-9 activity by SDS-PAGE zymography analysis. After treatment with actinonin, MMP-9 activity was reduced compared with placebo group. ^a $P < 0.05$ vs. placebo.

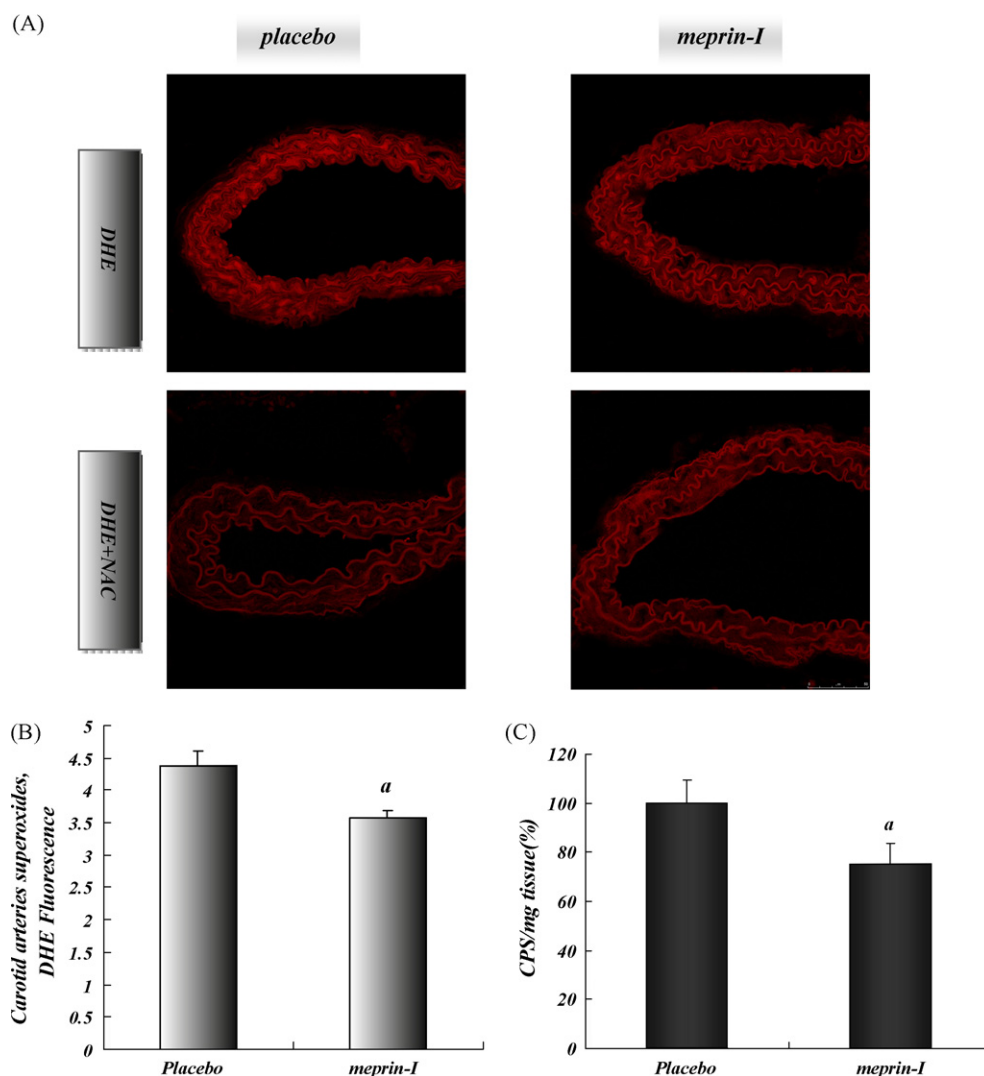


Fig. 5. Meprin-I decreases superoxide levels in carotid arteries and activity of NADPH oxidase. (A) Arterial-section superoxides were measured by staining with DHE with or without pretreatment with NAC. Bar = 50 μ m. (B) Superoxide-induced DHE signal is expressed as NAC-inhibited mean fluorescence for each mouse from saline-infused group (placebo) or actininin-infused group (meprin-I). Vertical bars are mean \pm SEM per group. (C) NADPH oxidase activity was assessed by 100 μ mol/L of NADPH-stimulated superoxide production detected with lucigenin-enhanced chemiluminescence, which was measured in counts per second (CPS) per milligram of tissue, and expressed as percentage of the mean value of the control group. ^a $P < 0.05$ vs. placebo.

Table 2
Effect of exogenous ANP and BNP on the behavior of macrophages and SMCs. Cell proliferation, apoptosis and ROS production were measured by ³H-Tdr incorporation assay, TUNEL assay and DCF-DA. SMCs = smooth muscle cells; THP-1 = THP-1 macrophage; ROS = reactive oxygen species. NEP-I = Neutral endopeptidase inhibition (cells treated with the NEP inhibitor candoxatrilat). Meprin-I = meprin inhibition (cells treated with the meprin inhibitor actininin). Data are mean \pm SEM.

Behavior/cell type	Control	ANP			BNP		
		ANP	+meprin-I	+NEP-I	BNP	+meprin-I	+NEP-I
Proliferation %							
SMCs	100 \pm 0	69 \pm 6 ^a	65 \pm 12 ^a	32 \pm 9 ^{a,b}	79 \pm 4 ^a	41 \pm 7 ^{a,c}	22 \pm 6 ^{a,c,d}
THP-1	100 \pm 0	105 \pm 2	92 \pm 3	86 \pm 6	82 \pm 5 ^a	55 \pm 4 ^{a,c}	31 \pm 3 ^{a,c,d}
Apoptosis %							
SMCs	100 \pm 0	43 \pm 7 ^a	48 \pm 3 ^a	23 \pm 6 ^{a,b}	69 \pm 8 ^a	41 \pm 4 ^{a,c}	18 \pm 2 ^{a,c,d}
THP-1	100 \pm 0	31 \pm 6 ^a	35 \pm 2 ^a	9 \pm 5 ^{a,b}	52 \pm 4 ^a	25 \pm 3 ^{a,c}	11 \pm 5 ^{a,c,d}
ROS production %							
SMC	100 \pm 0	63 \pm 4 ^a	55 \pm 5 ^a	43 \pm 2 ^{a,b}	82 \pm 5 ^a	62 \pm 4 ^{a,c}	15 \pm 6 ^{a,c,d}
THP-1	100 \pm 0	32 \pm 3 ^a	41 \pm 7 ^a	18 \pm 2 ^{a,b}	53 \pm 8 ^a	22 \pm 2 ^{a,c}	7 \pm 4 ^{a,c,d}

^a $P < 0.05$ vs. control.
^b $P < 0.05$ vs. ANP.
^c $P < 0.05$ vs. BNP.
^d $P < 0.05$ vs. BNP + actininin.

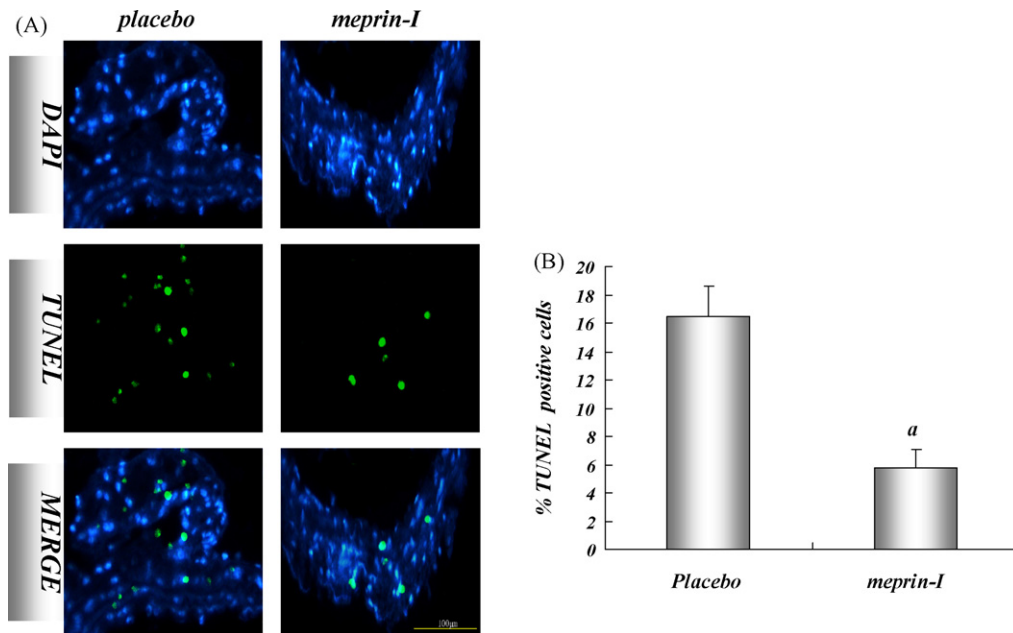


Fig. 6. (A) The number of TUNEL-positive nuclei is reduced in the carotid artery lesions of meprin-I ApoE^{-/-} mice. TUNEL analysis of sections of carotid arteries from placebo ApoE^{-/-} and ApoE^{-/-} mice treated with the meprin inhibitor actinonin for 6 weeks. Micrographs display nuclei (blue), TUNEL-positive signal (green), and merged images. Bar = 100 μm. (B) quantitative data of TUNEL-positive cells in sections of carotid arteries of ApoE^{-/-} mice treated with placebo and meprin-I. ^aP < 0.05 vs. placebo. (For interpretation of the references to color in this figure legend, the reader is referred to the web version of the article.)

3.5. *In situ* superoxide production, NADPH oxidase activity, and *in situ* cell death

To measure the effect of actinonin on superoxide levels in arteries, frozen sections from the carotid artery roots of actinonin-infused (meprin-I) and saline-infused (placebo) mice were stained with dihydroethidium (DHE) with or without pre-treatment with the superoxide scavenger N-acetyl L-cysteine (NAC; Fig. 4). Actinonin markedly suppressed superoxide levels in the carotid arteries of ApoE-deficient mice (24% decrease compared with saline-infused mice; Fig. 4). Consistent with decreased *in situ* production of ROS, NADPH oxidase activity was also significantly reduced in tissues from actinonin-treated ApoE^{-/-} mice (20% decrease compared with saline-infused mice; Fig. 5).

An increasing body of evidence suggests a major role for cell death in the progression and instability of atherosclerotic plaques. Numerous studies also link excess generation of ROS with cellular damage within atherosclerotic plaques. Fig. 6 shows cell death-associated DNA damage detected by TUNEL. Actinonin treatment significantly reduced the number of TUNEL-positive cells in the carotid arteries of ApoE^{-/-} mice fed a high-fat diet.

3.6. Apoptosis, proliferation, and migration of cells, and intracellular ROS production

Exogenous ANP failed to affect proliferation rates of THP-1 cells (Table 2). BNP significantly inhibited proliferation of THP-1 cells. Exogenous ANP and BNP significantly affected serum-induced VSMC proliferation compared with untreated cells (Table 2). Neutral endopeptidase inhibition (NEP-I) increased ANP- and BNP-inhibited VSMC proliferation rate, but actinonin increased only BNP-inhibited VSMC proliferation rate.

The rate of lipopolysaccharide-induced apoptosis, as detected by TUNEL assay in THP-1 cells and VSMC, was reduced by treatment with ANP and BNP compared with untreated cells (Table 2). NEP-I increased ANP- and BNP-inhibited cell apoptosis, and actinonin increased the effects of BNP on cell apoptosis only. These effects of

NEP-I and actinonin work in parallel with ROS production in VSMC and THP-1 cells.

4. Discussion

The present study demonstrated that meprin inhibition by actinonin suppresses the formation of atherosclerotic plaques, and preserves vascular wall function in ApoE^{-/-} mice fed a high-cholesterol diet. This suggests that meprin may play a significant part in atherosclerosis. Increased production of ROS has an important role in the initiation and progression of atherosclerosis. Investigations in cultured cells, animal models, and human studies have led to the identification of NAD(P)H oxidases as major sources of ROS production. In the current study, meprin inhibition for 6 weeks reduced ROS production and NAD(P)H oxidase activity in the vascular wall by 25%. Reduced oxidant stress may contribute to the anti-atherogenic effects of meprin inhibition. Apoptosis of VSMC, endothelial cells and macrophages may promote plaque growth, pro-coagulation and may induce rupture, the major consequence of atherosclerosis in humans. The fact that increased levels of ROS induce cell apoptosis has been demonstrated in these cells. In the present study, meprin inhibition also reduced apoptosis measured by an *in situ* cell death assay (TUNEL).

An increased extracellular matrix (ECM) is pathogenic in various chronic tissue injuries, but a reduced and/or disrupted ECM may be detrimental in atherosclerosis. The vascular remodeling that is thought to stabilize atherosclerotic plaques includes decreased lipid or cellular components but particularly increased ECM. Recent findings suggest that prevention of ECM degradation or even increasing ECM components such as collagen and elastin (“plaque stabilization”) improves outcome in atherosclerotic disease by decreasing the risk for plaque progression [25–27]. In the present study, treatment of ApoE^{-/-} mice with actinonin resulted in a dramatic reduction in lesion size, monocyte/macrophage content, and augmentation of collagen deposition. Actinonin significantly reduced the activity of MMP-9, suggesting a role of MMP-9 in actinonin regulation of collagen content. This may be consistent with a previous study by Galis et al. [28].

Meprin has been reported to hydrolyze and inactivate various endogenous growth factors, vasoactive peptides, cytokines, and extracellular matrix proteins, such as bradykinin, substance-P, angiotensin I, angiotensin II, NPs, and endothelin [6,7]. Meprin could therefore affect arterial responses to these endogenous vasoactive peptides circulating in the blood or produced in the peripheral arterial walls by regulating their local concentrations in the arterial walls. Systemic administration of drugs that inhibit meprin could increase levels of endogenous vasoactive peptides, which are cleaved by meprin, in the circulation or in peripheral tissues. Previous reports and the present study showed that actinonin administration induced elevation of levels of ANP and BNP, but not CNP, in serum in rats [8,9,12]. ANP and BNP, members of the NP family, are produced mainly in cardiomyocytes, but have also been found to be synthesized in VMSC, endothelial cells, and macrophages [29–32]. NPs have been shown to relax arterial smooth muscle and suppress proliferation of SMCs *in vitro*, and to inhibit intimal thickening of the carotid artery after intimal denudation *in vivo* [17,33,34]. NPs, which exist in the vascular endothelium and could be hydrolyzed by endothelial meprin, therefore exert anti-atherosclerotic effects on arterial walls. This scenario may be one of the mechanisms explaining the inhibition of formation of atherosclerotic plaques by actinonin administration. Demonstrating the *in vivo* increase of NPs or other cytokines in the circulation and in arterial tissues in ApoE^{-/-} mice fed cholesterol with actinonin is difficult because their expressions are very low and they act in an autocrine or paracrine manner.

The anti-atherogenic effects of actinonin were unlikely to be mediated mostly by ANP. Yamaguchi et al. [8] and Stephenson and Kenny [9] described ANP degradation by meprin-A but, when comparing the prominent ANP degradation by NEP, meprin was not the dominant ANP-degrading enzyme. The present study showed that actinonin administration decreased *in situ* production of superoxide and the activity of NADPH oxidases and apoptosis in carotid arteries. This may partly contribute to the mechanism(s) of the antioxidant effects of NPs because NPs were found to regulate ROS production in cardiomyocytes, VMSC, endothelial cells and macrophages [14,35–37]. In the present study, ANP and BNP were also found to suppress ROS production and apoptosis in THP-1 macrophages and primary cultured VSMC. NEP inhibition augments the effects of ANP and BNP's on different cell types, but actinonin only augments the effects of BNP with respect to ROS production, cell apoptosis and proliferation. This result may indicate that meprin inhibition exerts few anti-atherosclerotic effects by ANP. Meprin inhibition also increased the plasma and tissue concentrations of ANP, so we could not exclude the effects of ANP in the present study.

In conclusion, meprin has a significant role in atherogenesis, and meprin inhibition may be therapeutically useful in atherosclerosis prevention. Suppression of degradations in the arteries of endogenous NPs (or possibly other cytokines known to have anti-atherosclerotic actions) may at least partially contribute to the inhibitory effects of meprin inhibition on atherosclerotic changes. The precise mechanism for the inhibition of formation of atherosclerotic plaques due to the meprin inhibition merits further study.

Acknowledgements

The authors would like to thank Hua-Li Kang and Meng-Yang Deng for their excellent technical assistance, and also appreciate Dr. Jie Yu for her help *in vivo* experiments.

Funding: This study was supported, in part, by a grant (number 30770852) from the National Natural Science Foundation of China.

Appendix A. Supplementary data

Supplementary data associated with this article can be found, in the online version, at doi:10.1016/j.atherosclerosis.2009.04.036.

References

- [1] Bertenshaw GP, Norcum MT, Bond JS. Structure of homo- and hetero-oligomeric meprin metalloproteases. Dimers, tetramers, and high molecular mass multimers. *J Biol Chem* 2003;278:2522–32.
- [2] Bertenshaw GP, Villa JP, Hengst JA, Bond JS. Probing the active sites and mechanisms of rat metalloproteases meprin A and B. *Biol Chem* 2002;383:1175–83.
- [3] Bond JS, Rojas K, Overhauser J, Zoghbi HY, Jiang W. The structural genes, MEP1A and MEP1B, for the alpha and beta subunits of the metalloendopeptidase meprin map to human chromosomes 6p and 18q, respectively. *Genomics* 1995;25:300–3.
- [4] Norman LP, Jiang W, Han X, Saunders TL, Bond JS. Targeted disruption of the meprin beta gene in mice leads to underrepresentation of knockout mice and changes in renal gene expression profiles. *Mol Cell Biol* 2003;23:1221–30.
- [5] Tsukuba T, Kadowaki T, Hengst JA, Bond JS. Chaperone interactions of the metalloproteinase meprin A in the secretory or proteasomal-degradative pathway. *Arch Biochem Biophys* 2002;397:191–8.
- [6] Bond JS, Butler PE, Beynon RJ. Metalloendopeptidases of the mouse kidney brush border: meprin and endopeptidase-24.11. *Biomed Biochim Acta* 1986;45:1515–21.
- [7] Yamaguchi T, Kido H, Fukase M, Fujita T, Katunuma N. A membrane-bound metallo-endopeptidase from rat kidney hydrolyzing parathyroid hormone. Purification and characterization. *Eur J Biochem* 1991;200:563–71.
- [8] Yamaguchi T, Kido H, Katunuma N. A membrane-bound metallo-endopeptidase from rat kidney. Characteristics of its hydrolysis of peptide hormones and neuropeptides. *Eur J Biochem* 1992;204:547–52.
- [9] Stephenson SL, Kenny AJ. The metabolism of neuropeptides. Hydrolysis of peptides by the phosphoramidon-insensitive rat kidney enzyme 'endopeptidase-2' and by rat microvillar membranes. *Biochem J* 1988;255:45–51.
- [10] Kone BC. Molecular biology of natriuretic peptides and nitric oxide synthases. *Cardiovasc Res* 2001;51:429–41.
- [11] Schreiner GF, Protter AA. B-type natriuretic peptide for the treatment of congestive heart failure. *Curr Opin Pharmacol* 2002;2:142–7.
- [12] Pankow K, Wang Y, Gembardt F, et al. Successive action of meprin A and neprilysin catabolizes B-type natriuretic peptide. *Circ Res* 2007;101:875–82.
- [13] Arjona AA, Hsu CA, Wrenn DS, Hill NS. Effects of natriuretic peptides on vascular smooth-muscle cells derived from different vascular beds. *Gen Pharmacol* 1997;28:387–92.
- [14] Baldini PM, De Vito P, D'Aquilio F, et al. Role of atrial natriuretic peptide in the suppression of lysophosphatidic acid-induced rat aortic smooth muscle (RASMC) cell growth. *Mol Cell Biochem* 2005;272:19–28.
- [15] De Vito P, Di Nardo P, Palmery M, et al. Oxidant-induced pHi/Ca²⁺ changes in rat aortic smooth muscle cells. The role of atrial natriuretic peptide. *Mol Cell Biochem* 2003;252:353–62.
- [16] Li Y, Hashim S, Anand-Srivastava MB. Intracellular peptides of natriuretic peptide receptor-C inhibit vascular hypertrophy via Gqalpha/MAP kinase signaling pathways. *Cardiovasc Res* 2006;72:464–72.
- [17] Schirger JA, Grantham JA, Kullo JJ, et al. Vascular actions of brain natriuretic peptide: modulation by atherosclerosis and neutral endopeptidase inhibition. *J Am Coll Cardiol* 2000;35:796–801.
- [18] Barber MN, Kanagasundaram M, Anderson CR, Burrell LM, Woods RL. Vascular neutral endopeptidase inhibition improves endothelial function and reduces intimal hyperplasia. *Cardiovasc Res* 2006;71:179–88.
- [19] Sukhanov S, Higashi Y, Shai SY, et al. IGF-1 reduces inflammatory responses, suppresses oxidative stress, and decreases atherosclerosis progression in ApoE-deficient mice. *Arterioscler Thromb Vasc Biol* 2007;27:2684–90.
- [20] Alexander MR, Knowles JW, Nishikimi T, Maeda N. Increased atherosclerosis and smooth muscle cell hypertrophy in natriuretic peptide receptor A^{-/-}-apolipoprotein E^{-/-} mice. *Arterioscler Thromb Vasc Biol* 2003;23:1077–82.
- [21] Xu Y, Lai LT, Gabrilove JL, Scheinberg DA. Antitumor activity of actinonin *in vitro* and *in vivo*. *Clin Cancer Res* 1998;4:171–6.
- [22] Jiang F, Guo Y, Salvemini D, Dusting GJ. Superoxide dismutase mimetic M40403 improves endothelial function in apolipoprotein(E)-deficient mice. *Br J Pharmacol* 2003;139:1127–34.
- [23] Cuaz-Perolin C, Jguirim I, Larigauderie G, et al. Apolipoprotein E knockout mice over-expressing human tissue inhibitor of metalloproteinase 1 are protected against aneurysm formation but not against atherosclerotic plaque development. *J Vasc Res* 2006;43:493–501.
- [24] Galis ZS, Khatri JJ. Matrix metalloproteinases in vascular remodeling and atherogenesis: the good, the bad, and the ugly. *Circ Res* 2002;90:251–62.
- [25] Cheng XW, Kuzuya M, Sasaki T, et al. Increased expression of elastolytic cysteine proteases, cathepsins S and K, in the neointima of balloon-injured rat carotid arteries. *Am J Pathol* 2004;164:243–51.
- [26] Sukhova GK, Zhang Y, Pan JH, et al. Deficiency of cathepsin S reduces atherosclerosis in LDL receptor-deficient mice. *J Clin Invest* 2003;111:897–906.

- [27] Grainger DJ, Witchell CM, Metcalfe JC. Tamoxifen elevates transforming growth factor-beta and suppresses diet-induced formation of lipid lesions in mouse aorta. *Nat Med* 1995;1:1067–73.
- [28] Galis ZS, Johnson C, Godin D, et al. Targeted disruption of the matrix metalloproteinase-9 gene impairs smooth muscle cell migration and geometrical arterial remodeling. *Circ Res* 2002;91:852–9.
- [29] Lincoln TM, Wu X, Sellak H, Dey N, Choi CS. Regulation of vascular smooth muscle cell phenotype by cyclic GMP and cyclic GMP-dependent protein kinase. *Front Biosci* 2006;11:356–67.
- [30] Ander AN, Duggirala SK, Drumm JD, Roth DM. Natriuretic peptide gene expression after beta-adrenergic stimulation in adult mouse cardiac myocytes. *DNA Cell Biol* 2004;23:586–91.
- [31] Vollmar AM, Schulz R. Gene expression and secretion of atrial natriuretic peptide by murine macrophages. *J Clin Invest* 1994;94:539–45.
- [32] Westendorp RG, Draijer R, Meinders AE, van Hinsbergh VW. Cyclic-GMP-mediated decrease in permeability of human umbilical and pulmonary artery endothelial cell monolayers. *J Vasc Res* 1994;31:42–51.
- [33] Wei CM, Hu S, Miller VM, Burnett Jr JC. Vascular actions of C-type natriuretic peptide in isolated porcine coronary arteries and coronary vascular smooth muscle cells. *Biochem Biophys Res Commun* 1994;205:765–71.
- [34] Houben AJ, van der Zander K, de Leeuw PW. Vascular and renal actions of brain natriuretic peptide in man: physiology and pharmacology. *Fundam Clin Pharmacol* 2005;19:411–9.
- [35] Chiurchiu V, Izzi V, D'Aquilio F, et al. Brain natriuretic peptide (BNP) regulates the production of inflammatory mediators in human THP-1 macrophages. *Regul Pept* 2008;148:26–32.
- [36] Laskowski A, Woodman OL, Cao AH, et al. Antioxidant actions contribute to the antihypertrophic effects of atrial natriuretic peptide in neonatal rat cardiomyocytes. *Cardiovasc Res* 2006;72:112–23.
- [37] Furst R, Brueckl C, Kuebler WM, et al. Atrial natriuretic peptide induces mitogen-activated protein kinase phosphatase-1 in human endothelial cells via Rac1 and NAD(P)H oxidase/Nox2-activation. *Circ Res* 2005;96:43–53.